Design Solutions for the Solar Cell Interconnect Fatigue Fracture Problem*

G. R. Mon**
R. G. Ross, Jr.***

Jet Propulsion Laboratory,
California Institute of Technology

ABSTRACT

Mechanical fatigue of solar cell interconnects is a major failure mechanism in photovoltaic arrays. The authors recently published a comprehensive approach to the reliability design of interconnects together with extensive design data for the fatigue properties of copper interconnects. This paper extends the previous work, developing failure prediction (fatigue) data for additional interconnect material choices, including aluminum and a variety of copper-Invar and copper-steel claddings. An improved global fatigue function is used to model the probability-of-failure statistics of each material as a function of level and number of cycles of applied strain. Life-cycle economic analyses are used to evaluate the relative merits of each material choice. The copper-Invar clad composites demonstrate superior performance over pure copper. Aluminum results are disappointing.

INTRODUCTION

In two previous publications the authors presented a procedure for determining solar cell interconnect design and the degree of interconnect redundancy necessary to achieve minimum life-cycle cost of delivered energy (1, 2). A flow diagram of that procedure is presented in Figure 1.

In Figure 1, the box labeled Interconnect Failure Prediction represents a computational procedure for obtaining interconnect failure probabilities for alternative interconnect and module designs as a function of the number of strain cycles. The box labeled Array Degradation Analysis represents an algorithm that relates array power reduction to the fraction of failed interconnects; it is an application of the series-paralleling analysis of Ross (3).

*This paper presents the results of one phase of research conducted at the Jet Propulsion Laboratory, California Institute of Technology, for the U. S. Department of Energy, through an agreement with the National Aeronautics and Space Administration.

**Member of the technical staff, Flat-Plate Solar Array Project, Energy Technology Engineering Section.

***Engineering Sciences Manager, Flat-Plate Solar Array Project, and Supervisor, Photovoltaic Engineering Group, Energy Technology Engineering Section.

The box labeled Life-Cycle Energy Cost Analysis represents the procedure for calculating the life-cycle energy costs associated with alternative interconnect designs; this procedure also is from Ross (3, 4).

In this paper the failure prediction algorithm of the previous papers is upgraded with the introduction of a global fatigue-curve function that relates interconnect strain, number of imposed strain cycles, and probability of failure. This function is of the form

$$\Delta\epsilon = K \cdot f(p) \cdot N^b \qquad (1)$$

where

$\Delta\epsilon$ = interconnect strain range

N = number of imposed strain cycles

f(p) = a function that describes the parametric dependency of $\Delta\epsilon$ and N on the probability of interconnect failure

K, b = intercept and slope constants

The design examples and fatigue curve data in the previous publications were limited to OFHC copper interconnects; this paper extends the fatigue data base to include a variety of other interconnect materials including aluminum, two copper-Invar-copper claddings, and a copper-stainless steel-copper cladding.

The life-cycle cost algorithm is used to integrate the fatigue performance, cost, and electrical-loss data to allow accurate assessment of the

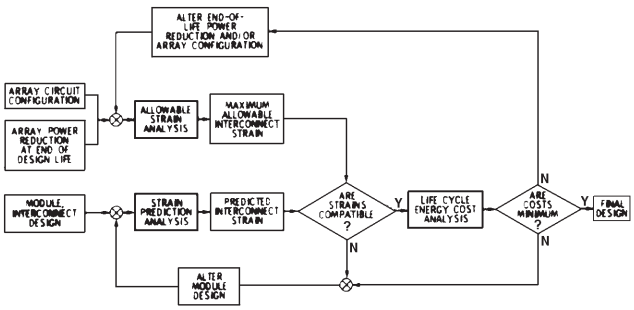

Fig. 1. Cost-Optimal Interconnect Reliability Design Algorithm

relative merits of the alternative interconnect materials.

FATIGUE PERFORMANCE

Fracture data for each of a variety of candidate interconnect materials were generated by mechanically cycling to failure several different sets of interconnect configurations at several different levels of strain range. The apparatus, procedure, interconnect configurations, and strain range computations were described earlier (1, 2). The raw data for each material are plotted as fracture probability vs cycles-to-failure at each test level of strain. One such plot, the OFHC copper data, is presented in Figure 2, within which are indicated schematically the several interconnect configurations tested.

Functional Modeling of Fatigue Data

The multivariate function expressed by Equation (1) is fitted to the complete data set for each material using a non-linear least squares minimization routine based upon the variable metric method of Davidon (5) as modified by Fletcher and Powell (6). The function f(p) is chosen as

$$f(p) = 10^{\sum_{i=0}^{3} a_i p^i} \qquad (2)$$

i.e., an exponential cubic polynomial. This function provided the best fit of several tried.

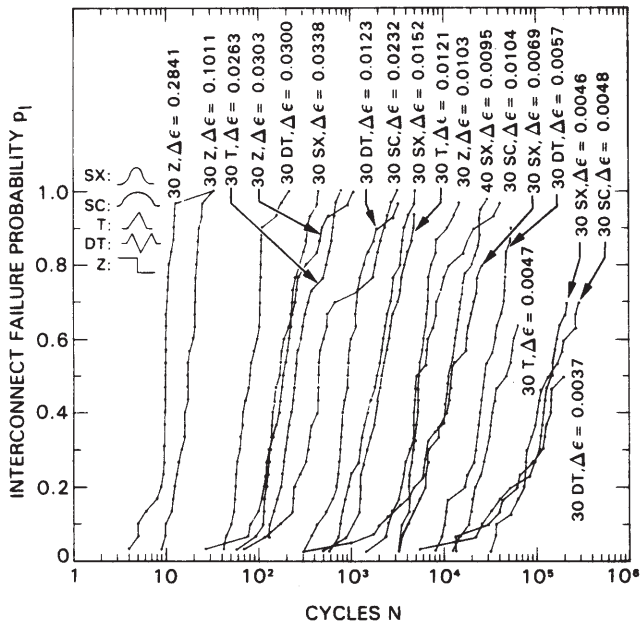

Fig. 2. Experimental Data: OFHC Copper Interconnects

The functional fatigue curves for the several candidate materials are plotted in Figure 3(a) to 3(e). It should be noted that the 33 CU/33 INV/33 CU material was tested in two metallurgical conditions (annealed and 20% cold-rolled) and two slitting orientations (parallel and transverse to the rolling direction) with no observed statistical difference in the results. The fatigue function presented here for this material includes a combination of data from the four cases.

Comparison of Fatigue Performance

In Table 1 the materials are identified and their fatigue performance is compared by listing, in the column labelled Y, the time to achieve 10% interconnect failures at the same strain level (hence thickness), which gives Y = 20 years for OFHC copper. The column headed Y/Y_{Cu} lists factors of improvement over copper.

It is evident that the cladding of copper with stronger metals can significantly improve its fatigue performance. The more ductile Invar is clearly a better choice than the more brittle stainless steel. In fact, a 33% Invar cross section gives about the same order of performance improvement as does a 68% stainless steel cross section. The fatigue performance superiority of Invar as an interconnect material was noted in an early study by Kaplan (7).

The fatigue performance of aluminum is not as good as that of copper. This fact and its poor solderability places aluminum at a definite disadvantage as an interconnect material.

Fracture Considerations

During the fatigue testing of the considered materials, some observations concerning the nature of crack initiation and propagation were noted that may be relevant to the design selection process.

It has generally been observed that cracks tend to initiate on the more highly stressed concave (lower) surfaces of the interconnect and tend to propagate through the thickness toward the less highly stressed convex (upper) surfaces. Many such microcracks coalesce to form the observed macrocrack.

This process is evident in the low-magnification SEM photographs in Figures 4(a) and 4(b), which show the two surfaces of a partially cracked copper-Invar clad interconnect; the formation of vertical microcracks ahead of the horizontal macrocrack is apparent.

Cracks starting on the more highly stressed surface will penetrate the thickness more deeply than will cracks that start on the less highly stressed surface. This process reduces the effective interconnect thickness during the crack propagation stage and shifts the neutral surface, along which final tearing occurs, toward the less highly stressed

surface. This is depicted schematicallly in Figure 5. A high-magnification SEM photograph, Figure 4(c), shows such a neutral surface as a line between the cladding interfaces, shifted toward the less highly stressed surface.

Figure 6 is a high-magnification SEM photograph of a tinned-aluminum fracture cross section. To be noted here and in Figure 4(c) is the observation that, apparently, interfacial layers such as a cladding boundary or a tinning interface may arrest crack propagation to a certain extent.

Since cracks initiate on surfaces, perhaps the stronger metals should form the surface layers of a clad-metal interconnect; this should be tested.

LIFE-CYCLE ENERGY COST ANALYSIS

Although fatigue is a key factor determining the merit of a candidate interconnect material, other factors such as material and installation costs and electrical resistivity must be considered before a final ranking can be determined. Comparison on the basis of cost contribution to the total life-cycle cost of delivered energy has been shown to provide an effective means of integrating these diverse performance factors. Following the authors' previous work (1-4), the life-cycle cost of delivered energy can be described by the following equation:

$$R = \frac{C_B + \frac{C_A + C_I + C_M}{\eta}}{I_0 \epsilon_{LC}} \qquad (3)$$

where

R = constant worth of energy over array lifetime, $/kWh

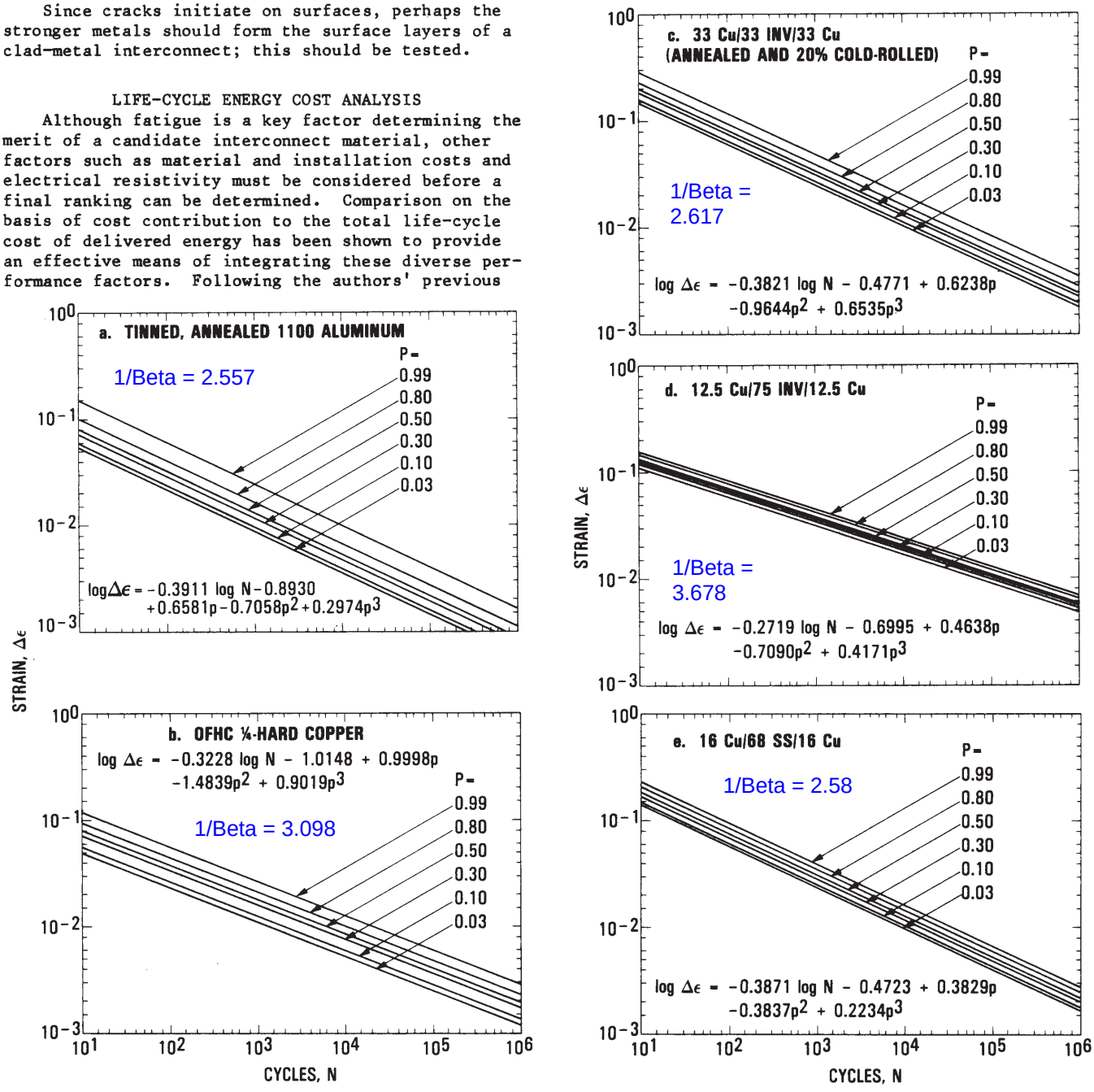

Fig. 3. Statistical Fatigue Function: Strain Range vs Number of Strain Cycles with Failure Fraction as Parameter

Table 1. Comparative Fatigue Performance of Candidate Interconnect Materials

Type of Material	Material Identification	Volumetric % Non-Cu Material	Y (years)	$\frac{Y}{Y_{Cu}}$
	Tinned 1100 aluminum		7.4	0.4
Homogeneous	Oxygen-free high-conductivity (OFHC) 1/4-hard copper	0.0	20.0	1.0
	33 Cu/33 INV/33 Cu	33.3	105.5	5.3
Cladding	12.5 Cu/75 INV/1.25 Cu	75.0	1031.5	51.6
	16 Cu/68 SS/16 Cu	68.0	84.7	4.2

INV = Invar: 36% Ni, 64% Fe;
SS = Type 430 stainless steel

C_B = balance of plant costs, \$/kW

C_A = initial array costs less interconnects, $\$/m^2$

C_I = add-on cost of interconnects per square meter of module area, $\$/m^2$

C_M = life-cycle operation and maintenance costs, $\$/m^2$

I_0 = annual solar insolation, $kWh/m^2/yr$

ϵ_{LC} = life-cycle energy fraction (1)

η = plant efficiency (at 100 mW/cm^2, NOCT)

The manner in which each interconnect material performance parameter influences the life-cycle cost is delineated in the following subsections.

Fatigue

The fatigue performance of a material influences the life-cycle cost through array power degradation due to open circuits [ϵ_{LC} in Equation (3)]. Values of ϵ_{LC} are determined by the array circuit configuration, the degree of interconnect redundancy, and the fraction p of failed interconnects over the array design life (20 years). The latter variable (p) is in turn determined by the fatigue characteristics of the interconnect material, as fixed by module design and site environment; i.e., p is determined, through the material fatigue function, by the strain range experienced by interconnects in the array field, and hence by the thickness of the interconnect.

Electrical Resistivity

The electrical resistivity of an interconnect material influences the life-cycle cost through I^2R

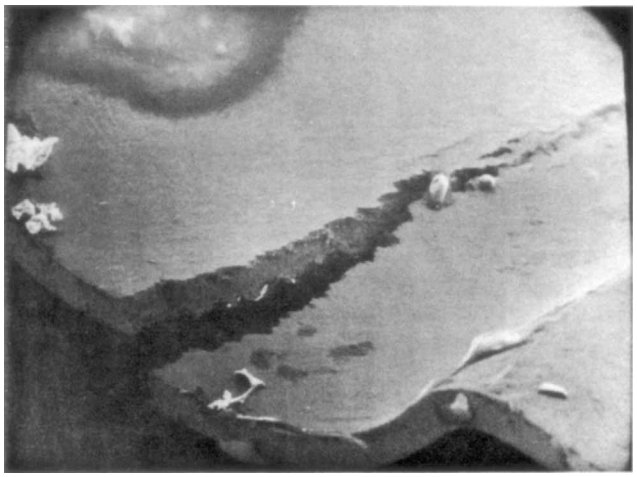

a. Concave Surface, 50X

b. Convex Surface, 20X

c. Cross-Sectional View, 5000X

Fig. 4. SEM Views of Partially Fractured 12.5 Cu/75 INV/12.5 Cu Interconnect

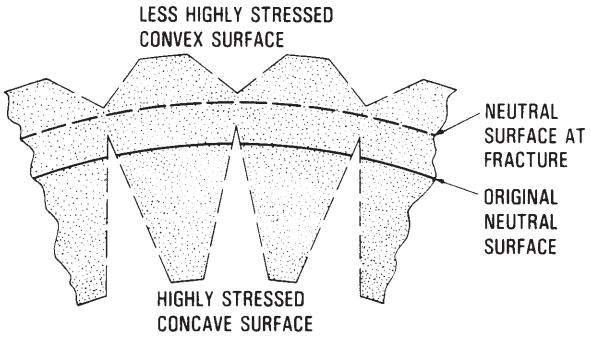

Fig. 5. Schematic for Explaining Fatigue Crack Propagation in Interconnects

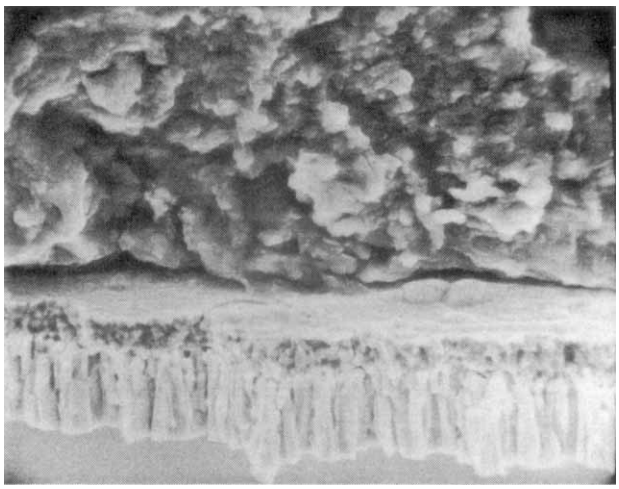

Fig. 6. SEM Photograph of Tinned Aluminum Fracture: Cross Section, 2000X

losses [η in Equation (3)]. The interconnect power-loss efficiency will depend upon the materials used, the cladding ratio (if the interconnect material is a cladding), the width, and the thickness. The impact of these factors on cost is explicitly recognized in the following expression for plant efficiency:

$$\eta = \eta_0\left(1 - \frac{I^2\Omega}{P_0}\right)\left(1 - \frac{LW}{A}\right) \qquad (4)$$

where

η_0 = baseline plant efficiency

I = solar cell current at maximum power, amperes

P_0 = cell power output, watts

Ω = interconnect effective resistance, ohms

L = length of interconnect over cell, in.

w = total interconnect width, in.

A = cell area, $in.^2$

In Equation (4) the first expression in parentheses is the interconnect power loss efficiency; the second expression is the cell power loss efficiency resulting from coverage by interconnects.

The resistance Ω is given by

$$\Omega = \frac{\ell\rho}{wt} \qquad (5)$$

where

ℓ = interconnect effective length, in.

w = total interconnect width, in.

t = interconnect thickness, mils

ρ = interconnect material resistivity, ohm-mils

For a clad-metal interconnect consisting of metals in the volumetric, or thickness, ratio x/y/x,

$$\rho = \rho_x \frac{1}{2x + y\left(\frac{\rho_x}{\rho_y}\right)} \qquad (6)$$

where

ρ_x = electrical resistivity of material x, ohm-mils

ρ_y = electrical resistivity of material y, ohm-mils

Cladding ratios and resistivity parameters for the candidate interconnect materials are presented in Table 2 for use in Equations (5) and (6).

Cost

The cost of interconnects influences life-cycle energy costs by the term C_I in Equation (3).

Cost Analysis Example

Cost/performance comparisons among candidate interconnect materials are developed here for equal

Table 2. Cladding Ratios and Resistivities of Candidate Interconnect Materials

Sample Material	x	y	(ρ_{Cu}/ρ_y)	$\rho \times 10^{-6}$
Tinned Aluminum	0	1.0	0.58	1148.52
OFHC Copper	0.5	0	1.00	666.14
33 Cu/33 INV/33 Cu	0.33	0.33	0.18	916.71
12.5 Cu/75 INV/12.5 Cu	0.125	0.750	0.18	1730.23
16 Cu/68 SS/16 Cu	0.16	0.68	0.03	1956.93

total interconnect width (cell loss due to shading), effective interconnect length, module design, array circuitry, and site environment. The same series-parallel array circuit model as used previously (1, 2) is used here, as reflected in the tabulation of ϵ_{LC} values in Table 3.

Material, labor, and overhead costs in 1980 dollars are presented in Figure 7(a) to 7(e). These were compiled from supplier quotations and other sources (8) by Burger (9).

Other constants used in the analysis are presented below:

C_B = 250 \$/kW

C_A = 113 \$/m^2

C_M = 0

I_O = 2000 kWh/m^2/yr

$\eta_O(1 - \frac{LW}{A})$ = 0.092

I = 2.0 amps

P_O = 1.2 watts

ℓ = 3.0 in.

w = 0.2 in.

Cost Analysis Results

The results of the cost analysis are presented in Figure 8(a) to 8(e) in terms of the fractional increment in life-cycle energy cost due to interconnects, denoted as Γ:

$$\Gamma = \frac{\Delta R}{R_0} = \frac{R - R_0}{R_0} \qquad (7)$$

Table 3. Life-Cycle Energy Fractions

20-Year Cumulative Interconnect Failure Probability	Life-Cycle Energy Fraction ϵ_{LC}					
P_I	r = 1	2	3	4	5	6
0.005	17.8	19.95	20	20	20	20
0.010	16.6	19.90	19.96	20	20	20
0.050	11.7	19.45	19.89	19.98	20	20
0.100	7.7	18.2	19.76	19.92	19.98	20
0.150	4.4	16.5	19.55	19.88	19.96	20
0.200	2.25	13.2	18.47	19.55	19.88	20
0.300	1.74	11.2	17.1	18.65	19.66	19.91
0.400	1.60	9.9	15.17	17.1	18.7	19.15
0.500	1.5	8.9	13.2	15.6	17.4	17.9

where

R = calculated life-cycle energy cost from Equation (3)

R_0 = ideal life-cycle energy cost assuming cost-free and loss-free interconnects (i.e., life-cycle energy cost without interconnects)

Figure 8(a) to (e) are plots of Γ for each material vs interconnect thickness (and strain) with interconnect redundancy as the parameterizing variable. The fractional life-cycle cost increment Γ fully incorporates the initial cost of interconnect materials and installation, the I^2R electrical efficiency losses, and array energy degradation from interconnect fatigue failures (open circuits).

The plots are seen to have common features. The dashed lines give life-cycle cost increments for fatigue-free, but not cost-free, interconnects. The solid lines give cost increments considering all losses, including those due to fatigue effects, which, once a critical thickness or strain level is exceeded, increase rapidly. For thicknesses well below that critical level, resistivity effects (I^2R losses) dominate the incremental costs. A minimum in the incremental cost occurs between these extremes and is the suggested design point, since at this point the incremental life-cycle costs are least sensitive to variations in thickness or strain.

The sensitivity to random, non-fatigue-related failures, taken as 1 per 200 in 20 years, is dramatic for a single interconnect, as evidenced by the large disparity between incremental costs for modules with no interconnect redundancy, see Figure 8. For two or more interconnects, this sensitivity essentially disappears. This emphatically suggests the use of at least two interconnects per cell. Interconnect redundancies greater than two tend to allow more thickness margin but at a higher cost penalty.

From Figure 8(b), for OFHC copper, two 1.5-mil-thick interconnects or three 2.0-mil thick interconnects will limit the life-cycle cost contribution to about 5%. From Figure 8(a) it is seen that aluminum cannot compete with copper -- there is little thickness design margin and resulting cost contributions exceed 5%.

From Figure 8(c) it is observed that the 33 Cu/33 INV/33 Cu is fully cost-competitive with copper at double redundancy for thicknesses less than 4.0 mils; in fact, the flatness of the cost minimum assures insensitivity to thickness variation that may result during the fabrication process, an advantage that copper lacks.

The remaining copper-Invar clad material, Figure 8(d), exhibits desirable minima at 3.0 mils but, for double redundancy, at a slightly higher cost penalty: 7%. The copper-stainless steel clad interconnect, Figure 8(e), is likewise more expensive.

The above design solution is specific for a particular module construction and site environment (1, 2). These factors determine the proportionality between interconnect strain and thickness. For this example, the proportionality was chosen so that at a strain level $\Delta\epsilon = 0.0055$, 2.0-mil copper interconnects give five failures per thousand ($p = 0.005$) in 20 years. This fixes the critical copper interconnect thickness at 2.0 mils and the corresponding 33 Cu/33 INV/33 Cu critical thickness at 4.0 mils.

Uncertainty Analysis

Because at the critical thickness small variations in strain can result in large cost penalties, it is prudent to provide some design margin. How much margin is sufficient is revealed by an uncertainty analysis.

Factors influencing the computation of interconnect strain lead to an uncertainty in that quantity of about 20%. Use of the function-fitting routine results in an average rms error of 0.24 of a log cycle due to scatter in the experimental data; this results in a 30% uncertainty in strain level for a given level of failure and number of cycles of applied strain. The total uncertainty of about 50% suggests that the design thickness be chosen at about half the critical thickness. Fortunately, this corresponds closely to the life-cycle cost minimum.

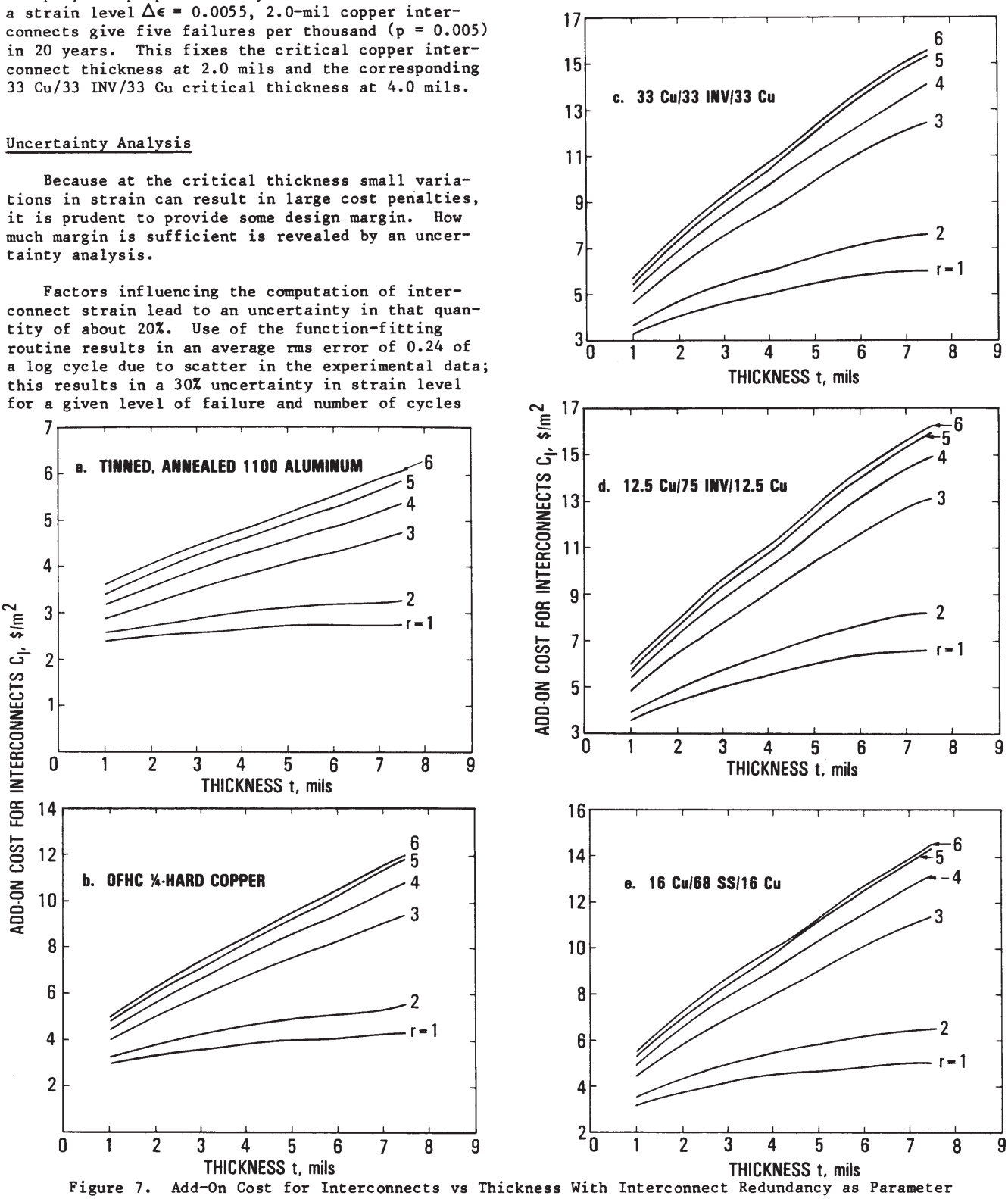

Figure 7. Add-On Cost for Interconnects vs Thickness With Interconnect Redundancy as Parameter

CONCLUSIONS

Comparative fatigue, cost, and electrical performance testing and analysis of aluminum, copper, and copper-clad interconnects, reveal that copper and 33 Cu/33 INV/33 Cu give superior total performance at low levels of interconnect redundancy. Aluminum performance is disappointing.

The life-cycle cost analysis algorithm, incorporating interconnect material costs and fatigue and electrical performance, has been demonstrated to be an effective interconnect design selection procedure.

ACKNOWLEDGEMENTS

The authors wish to extend thanks to Solarex Corp. and Texas Instruments Corp. for supplying

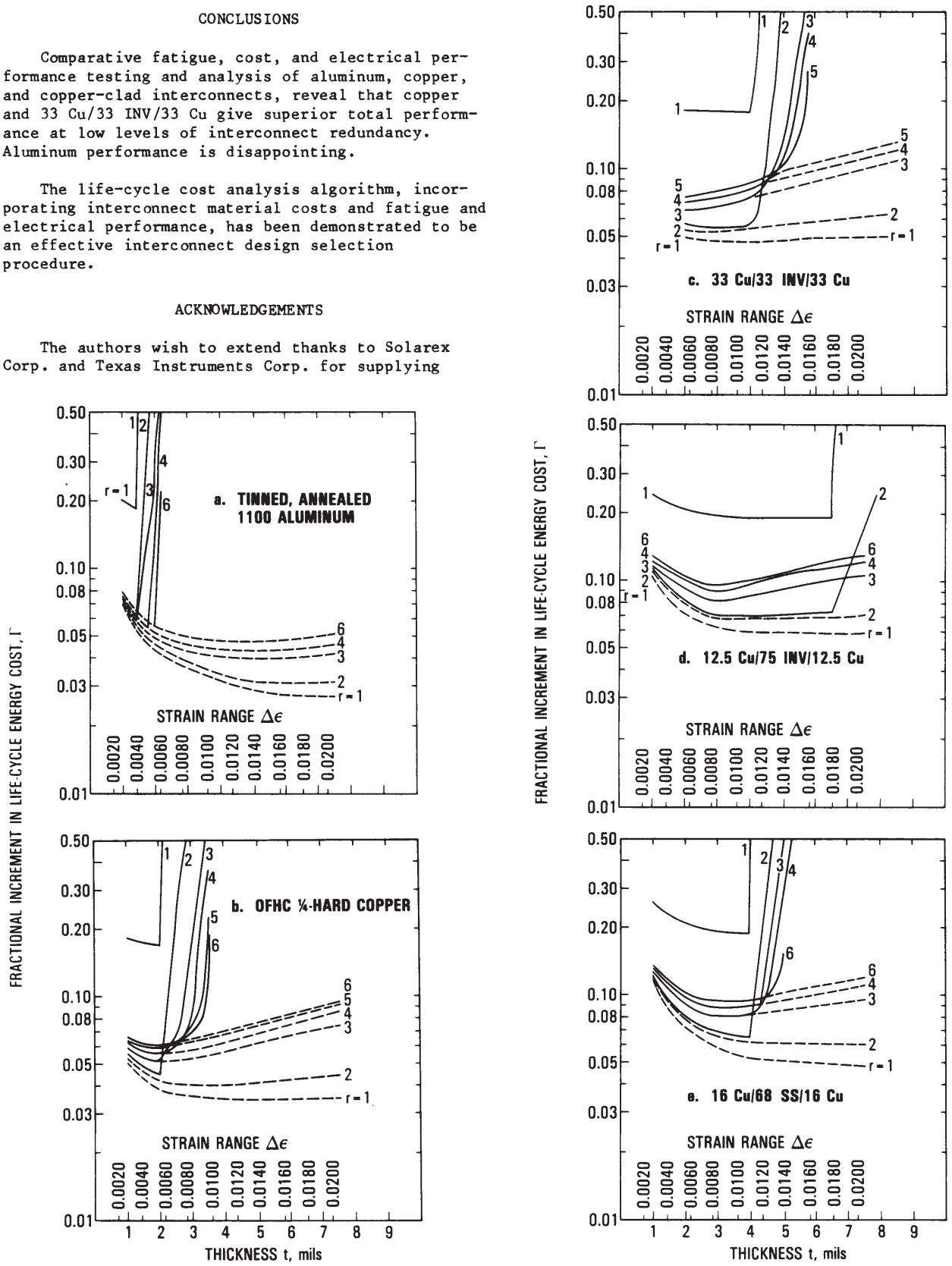

Figure 8. Fractional Increment in Life-Cycle Energy Cost Due to Interconnects vs Thickness, With Interconnect Redundancy as Parameter

interconnect materials, to E.S. Jetter and T. Sullivan for conducting tests, to D.R. Burger for his many contributions, to K.C. Evans for the electron micrographs, and to G.M. Hill for executing the computer runs.

REFERENCES

1. Mon, G.R., Moore, D.M., Ross, R.G., Jr., Interconnect Fatigue Design for Terrestrial Photovoltaic Modules, JPL Publication 81-111, JPL Document No. 5101-173, Jet Propulsion Laboratory, Pasadena, California, March 1982.

2. Mon, G.R., Moore, D.M., Ross, R.G., Jr, "Solar Cell Interconnect Design for Terrestrial Photovoltaic Modules," Fourth A.S.M.E. Solar Division Annual Technical Conference, Albuquerque, New Mexico, April 1982.

3. Ross, R.G., Jr., "Flat-Plate Photovoltaic Array Design Optimization," Proceedings of the 14th IEEE Photovoltaic Specialists Conference, pp. 1126-1132, 1980.

4. Ross, R.G., Jr., "Photovoltaic Design Optimization for Terrestrial Applications," Proceedings of the 13th IEEE Photovoltaics Specialists Conference, pp. 1067-1073, 1978.

5. Davidon, W.C., "Variable Metric Method for Minimization," AEC R&D Report ANL-5990, 1959.

6. Fletcher, R., and Powell, M.J., "Rapidly Convergent Descent Method for Minimization," Computer Journal, Vol. 7, pp. 149-154, July 1964.

7. Kaplan, A., "Fatigue Analysis of Solar Cell Welds," Conference Record of the Tenth IEEE PV Specialists Conference, pp. 281-286, 1973.

8. Chamberlain, R.G., and Aster, R.W., SAMICS Input Data Preparation, JPL Document No. 5101-44 (Revision B), April 1980.

9. Burger, D., private communication.